International Conference on Hydroinformatics

2014

Effect Of Sediment Releasing Operation From Reservoir Outlets On The Water Treatment Plant Downstream

Jihn-Sung Lai

Fong-Zuo Lee

Cheng-Chia Huang

Gwo-Wen Hwang

Shang-Shu Shih

See next page for additional authors

Authors

Jihn-Sung Lai, Fong-Zuo Lee, Cheng-Chia Huang, Gwo-Wen Hwang, Shang-Shu Shih, Wen-Da Guo, Chia-Hui Chou, and Yih-Chi Tan

EFFECT OF SEDIMENT RELEASING OPERATION FROM RESERVOIR OUTLETS ON THE WATER TREATMENT PLANT DOWNSTREAM

J. S. LAI(1,2,3), F. Z. LEE(3), C. C. HUANG(1) , G. W. HWANG(2), S. S. SHIH(2), W. D. GUO(4) , C. H. CHOU(5), Y. C. TAN(1,2,3)

(1): Hydrotech Research Institute, National Taiwan University, TAIWAN, R.O.C.

(2): Dept. of Bioenvironmental Systems Eng., National Taiwan University, TAIWAN, R.O.C.

(3): Center for Weather Climate and Disaster Research, TAIWAN, R.O.C.

(4): Taiwan Typhoon and Flood Research Institute National Applied Research Laboratories Taipei, Taiwan, R.O.C.

(5): Northern Region Water Resources Office, Water resources agency, Ministry of Economic Affairs, TAIWAN, R.O.C.

ABSTRACT

With steep slope and strong rainfall intensity, landslide and debris flow could generate huge amount of sediment yield from the watershed, typically during typhoon floods in Taiwan. As huge amount of sediment moving into a reservoir, serious sedimentation problem could reduce storage of reservoir due to decrease of flow velocity and lack of sufficient sediment releasing bottom outlet. Therefore, using flood discharge to release sediment during Typhoon or rain fall duration is very important. This study adopts the data of field observation at outlet structures of the Shihmen reservoir to establish the operational strategies of sediment releasing rule for providing secured water supply at downstream river intake. Based on the numerical simulation by using 2D model coping with field data, the relationship of sediment concentration between the Shihmen reservoir and downstream withdraw intake at the Yuanshan weir can be established. The sediment concentration reduction ratio is calculated to be 89% from the Shihmen reservoir to the Yuanshan weir. This study also focuses on the reduction of sediment concentration released from bottom outlet by adding clear water from the tunnel spillway. From simulated results, when the extra discharge of tunnel spillway reaches 830m^3/s in a specific event, the influence of reducing sediment concentration to downstream river by opening tunnel spillway can maintain water supply of downstream withdraw intake at Yuanshan weir. In practiceal cases, when using the added water from tunnel spillway to reduce sediment concentration during Typhoon Haitang and Typhoon Wipha, the sediment concentration at Yuanshan weir can reduce water turbidity lower than 6000NTU that can be treated by water treatment plant.

Keywords: Sediment releasing; Downstream withdraw intake; Sediment concentration; Water supply.

INTRODUCTION

The sustainable operation and storage reservation of existed reservoir is going to be a vital issue due to reservoir sedimentation is already higher than the increase of reservoir capacity by construction. Taiwan is situated at a geographical location with special climatic condition that brings to the Island 3.6 typhoons per annum on the average. In recent years, the numbers of typhoon is increasing to five. These typhoons often result in flood disasters that can cause serious damage to properties and sometimes with severe casualties. On the other hand, when typhoon or heavy rain fall occurs in Taiwan, the watershed may generate amount of sediment yield. And, land development in the watershed could accelerate soil erosion. As sediment moves into a reservoir, deposition occurs due to decrease of velocity. In general, the large size sediment may deposit quickly to form delta near the backwater region tail. The hydraulic phenomenon of delta area is similar to the shallow water of open channel. The inflow sediment presents two patterns, bed load and suspended load. The bed load may deposit at the front set of delta, and the suspended load may flow through the delta and deposit by sorting. When turbid inflow continues to move, the turbulence energy decreases by resistance. The inflow may plunge into the reservoir to develop turbidity current and move toward downstream. When turbidity current arrived at dam site, the flow would climb up along the dam slope. If gravity force, resistance and inertial force were equilibrium, the flow would stop to climb and started to drop. Then, the positive surge developed and moved to upstream. Finally, the reservoir would become turbid [6]. If lower sluiceway facility could be operated in time, the turbid flow would be flush out and reduce sediment deposit. However, if the outflow discharge was insufficient, the desiltation efficiency would be discounted and the sediment would deposit. In addition, when high turbid water was released to downstream river, the deposition effect and water quality effect were seriously affected [1].

Therefore, the Shihment reservoir was adopted as research area in this study. The data of field observation from outlet structures of the Shihmen reservoir were used to establish the operational strategies of sediment releasing rule and keep water sustained supply at downstream river intake at Yuanshan weir. Based on the numerical simulation by using 2D model coping with field data, the relationship of sediment concentration between the Shihmen reservoir and downstream withdraw intake at the Yuanshan weir can be established.

DESCRIPTION OF RESEARCH AREA

The Shihmen reservoir has a natural drainage area of 762.4 km^2. It is formed by the Shihmen dam located at the upstream reach of the Dahan River. The Dahan River is one of the three tributaries of the Tamshuei River which flows westward the Taiwan Strait. A map of the watershed area of the Shihmen reservoir is presented in figure 1. The figure 1 also showed the water intake was located at downstream river at Yuanshan weir. The Shihmen dam was constructed in 1963 is a 133.1m high embankment dam with spillways, permanent river outlet, power plant intake and flood diversion tunnels controlled by tailrace gates. The elevations of the spillway crest, permanent river outlet, power plant intake and flood diversion tunnels are EL.235 m, EL.169.5m, EL.173m and EL.220m, respectively. The total discharge of spillways is 11,400 m^3/s, permanent river outlet is 34 m^3/s, power plant intake is 137.2 m^3/s and flood diversion tunnels is 2,400 m^3/s. With a maximum water level of EL.245 m, the reservoir pool is about 16.5 km in length and forms a water surface area of 8.15 km^2. The initial storage capacity was 30,912x 10^5 m^3, and the active storage was 25,188x 10^5 m^3. Due to a lack of sufficient desiltation facilities, incoming sediment particles have settled down rapidly along the reservoir since the dam was completed. Based on the survey data, the Shihmen reservoir has accumulated a significant amount of sediment after dam completion. The depositional pattern has become wedge-shaped since 2000. From recent survey data in 2013, the storage capacity was estimated to be 70.24% of its initial capacity [7]. Based on the survey data, the longitudinal bed profile along the reservoir is plotted in Figure 2. As shown in Figure 2, the Shihmen reservoir has accumulated a significant amount of sediment after dam completion. The Figure 3 presents the sediment size distribution and the figure shows the sediment distribution is uniform. Based on sediment size distribution, the sediment classify in reservoir is closed to silt or clay [5].

NUMERICAL MODEL

The conservation system of governing equations are:

$$\frac{\partial \mathbf{Q}}{\partial t}+\frac{\partial \mathbf{F}_{\text{conv}}}{\partial x}+\frac{\partial \mathbf{G}_{\text{conv}}}{\partial y}=\frac{\partial \mathbf{F}_{\text{diff}}}{\partial x}+\frac{\partial \mathbf{G}_{\text{diff}}}{\partial y}+\mathbf{S} \tag{1}$$

in which

$$\mathrm{Q}=\begin{bmatrix} h \\ hu \\ hv \end{bmatrix},\ \mathrm{F}_{\text{conv}}=\begin{bmatrix} hu \\ u^2+gh^2/2 \\ huv \end{bmatrix},\ \mathrm{G}_{\text{conv}}=\begin{bmatrix} hv \\ huv \\ hv^2+gh^2/2 \end{bmatrix},$$

$$\mathrm{F}_{\textbf{diff}}=\begin{bmatrix} 0 \\ \frac{hT_{xx}}{\rho} \\ \frac{hT_{xy}}{\rho} \end{bmatrix},\ \mathrm{G}_{\textbf{diff}}=\begin{bmatrix} 0 \\ \frac{hT_{xy}}{\rho} \\ \frac{hT_{yy}}{\rho} \end{bmatrix},\ \mathrm{S}=\begin{bmatrix} 0 \\ gh\,(s_{0x}-s_{\text{f}\,x}) \\ gh\,(s_{0y}-s_{\text{f}\,y}) \end{bmatrix} \tag{2}$$

where $\mathbf{Q}$ is the conserved physical vector; $\mathbf{F}_{\text{conv}}$ and $\mathbf{G}_{\text{conv}}$ are the convection flux vectors in the *x*- and *y*-directions, respectively; $\mathbf{F}_{\text{diff}}$ and $\mathbf{G}_{\text{diff}}$ are the diffusion flux vectors in the *x*- and *y*-directions, respectively; $\mathbf{S}$ is the source term; h is the water depth; u and v are the depth-averaged velocity components in the *x*- and *y*-directions, respectively; g is the gravitational acceleration; $s_{0x}=-\partial z_b/\partial x$ and $s_{0y}=-\partial z_b/\partial y$ are the bed slopes in the *x*- and *y*-directions, respectively; z_b is the bed elevation; $s_{\text{f}\,x}$ and $s_{\text{f}\,y}$ are the friction slopes in the *x*- and *y*-directions, respectively; and T_{xx}, T_{xy} and T_{yy} are the depth-averaged turbulent stresses. The friction slopes are estimated according to the following Manning formula:

$$s_{\text{f}\,x}=\frac{un_{\text{Mann}}^2\sqrt{u^2+v^2}}{h^{4/3}},\ s_{\text{f}\,y}=\frac{vn_{\text{Mann}}^2\sqrt{u^2+v^2}}{h^{4/3}} \tag{3}$$

where n_{Mann} is the Manning roughness coefficient. The turbulent shear stresses are determined by the Boussinesq's assumption:

$$T_{xx}=\frac{2\rho\mu_t}{h}\frac{\partial(hu)}{\partial x},\ T_{xy}=\frac{\rho\mu_t}{h}[\frac{\partial(hu)}{\partial y}+\frac{\partial(hv)}{\partial x}],\ T_{yy}=\frac{2\rho\mu_t}{h}\frac{\partial(hv)}{\partial y} \tag{4}$$

where μ_t is the eddy viscosity due to turbulence, calculated by $\mu_t = 1/6\kappa u_* h$; κ is the von Karman coefficient of 0.4; $u_* = (\sqrt{(\tau_{bx}^2 + \tau_{by}^2)} / \rho)^{1/2}$ is the bed shear velocity; and $\tau_{bx} = \rho g h s_{fx}$ and $\tau_{by} = \rho g h s_{fy}$ are the bed shear stresses in the *x*- and y-directions, respectively.

For the numerical discretization, a scheme called FMUSTA (finite-volume multi-stage) (Guo et al., 2008) is adopted to estimate the numerical flux through each cell interface in the framework of finite volume method. In the treatment of source terms, the hydrostatic reconstruction method (HRM) is employed to prevent the imbalance between flux gradients and source terms. The presented 2D numerical model is practically suitable for complex flow conditions (mixed regimes) and also appropriate for special problems related to wetting and drying. The detailed description of the numerical formulation is given in Guo et al., (2011).

RESULT AND DISCUSSION

This study collects historical data of sediment concentration data of reservoir outlets and Yuanshan weir. The collection data includes 10 historical events. According to the historical records, typhoon Aere attacked northern Taiwan and caused substantial losses in 2004. Typhoon Aere brought into Tamshui River Basin a total rainfall of 973mm in 4 days (about 40% of the mean annual rainfall of the Basin). The excessive rainfall induced serious landslides in an area of 265 ha in the Shihmen reservoir watershed. This generated high sediment concentration in the runoff entering the reservoir. In the Typhoon Aere induced event, the turbidity at lower level of Shihmen Reservoir reached 326,700 NTU, which is far-beyond the maximum turbidity that water treatment plants at downstream river can handle. Due to the limitation of the water conveying capacity, the water treatment plants in neighboring counties can only support limited amount of water needed. So, the high sediment concentration problem is serious, not only public water supply but also sediment deposition problem. In 2005, another three typhoons attacked Shihmen reservoir which included Typhoon Haitang, Typhoon Matsa and Typhoon Talim. The maximum sediment concentration near the dam site of Typhoon Haitang, Typhoon Matsa and Typhoon Talim were 37,530NTU, 62,505NTU and 96,400NTU, respectively. In 2007 and 2008, the maximum sediment concentration near the dam of typhoon Typhoon Sepat and Typhoon Jangmi were 53,547 and 36,947 NTU, respectively. They are similarly brought sediment problem and the inflow concentration exceeded water treatment capacity of the plant which can only deal with 6,000 NTU [1].

The collection data were adopted to verify and calibrate 2D numerical model. After numerical model was verified and calibrated, the other historical events of reservoir outlets were used in boundary condition for the sediment concentration simulation at Yuanshan weir. Then, coping with simulation results and field measured data at Yuanshan weir, the sediment concentration reduction ratio is calculated to be 89% from the Shihmen reservoir to the Yuanshan weir, as shown in Figure 4. It means that if the water treatment capacity is limited to 6,000NTU, the sediment concentration of reservoir outlets is constrained to 6,742NTU. Based on this relationship, the sediment releasing operation with sustainable water withdraw at downstream intake can be modified from original operation using extra outflow discharge of tunnel spillway as shown in Figure 5. The Figure 5 shows the effect of sediment concentration due to various outflow discharges of tunnel spillway. Based on the effects of outflow discharge of tunnel spillway, the historical events of sediment releasing operation during Typhoon Wipha and Typhoon Haitang were investigated. The Figure 6 and Figure 7 show the changing patterns of outflow sediment concentration against with time using outflow discharge of tunnel spillway. According to the outflow sediment variation, the condition of sustainable water withdraw at downstream intake is to release extra discharge 440 m^3/s of tunnel spillway.

AKCNOWLEDGEMENT

The presented study was financially supported by the Northern Water Resources Bureau, Water Resources Agency Ministry of Economic Affairs. Writers wish to thank the Hydrotech Research Institute at National Taiwan University for technical support.

REFERENCES

[1] F. Z. Lee, J. S. Lai, W. D. Guo, C. C. Huang, F. J. Chang and Y. C. Tan "The impacts of water withdraw at Yuanshanyan during sediment venting in Shihmen Reservoir", Vol. 5, No. 4., (2012), pp. 80-94. (in Chinese).

[2] W. D. Guo, J. S. Lai, and G. F. Lin "Finite-volume multi-stage schemes for shallow-water flow simulations.", International Journal for Numerical Methods in Fluids, Vol. 57,(2008), pp. 171-204.

[3] W. D. Guo, J. S. Lai, and G. F. Lin, F. Z. Lee, and Y. C. Tan, "Finite-volume multi-stage scheme for advection-diffusion modeling in shallow water flow.", Journal of Mechanics, Vol. 27, No.3, (2011), 415-430.

[4] W. D. Guo, J. S. Lai, and G. F. Lin "Finite-volume multi-stage schemes for shallow-water flow simulations", Int. J. Numer. Meth. Fluids, Vol. 57, (2008), pp. 177-204.

[5] Hydraulic Planning and Experimental Institute, Water Resources Agency, Ministry of Economic Affairs "The observation and measurement of sediment transport and the studies of application and development of density current simulation model in Shihman Reservoir", National Chiao Tung University, (2008). (in Chinese)

[6] Northern water resources bureau, Water resources agency, Ministry of Economic Affairs "Research of arrangement and planning on depsition sediment in Shihmen Reservoir", (2010). (in Chinese).

[7] Northern water resources bureau, Water resources agency, Ministry of economic affairs "Reservoir sedimentation survey of Shihmen Reservoir", (2013). (in Chinese).

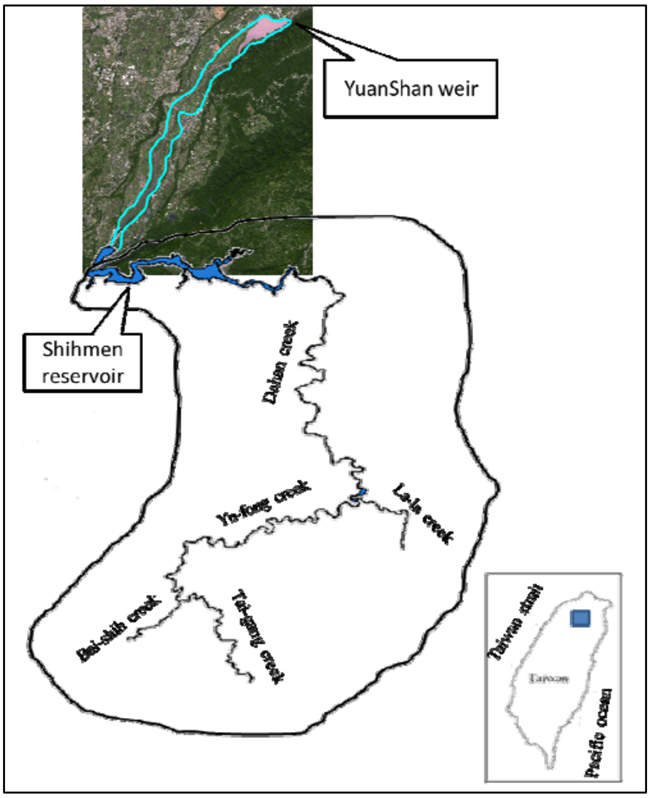

Figure 1. Shihmen reservoir watershed and sketch of research area

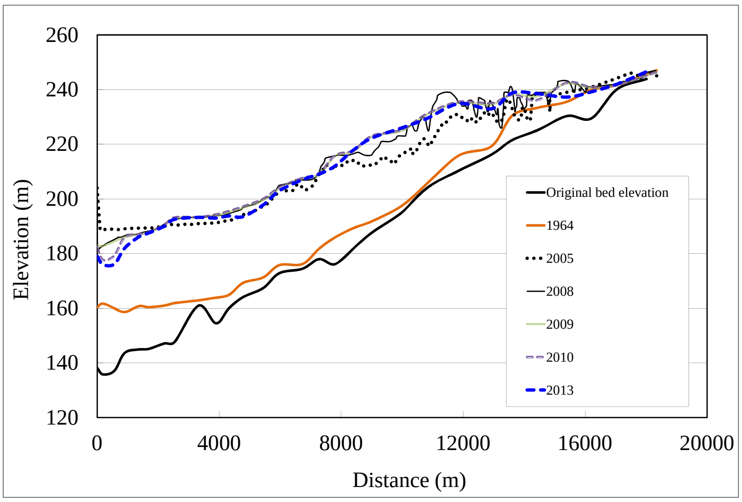

Figure 2 Longitudinal bed elevation of Shihmen reservoir

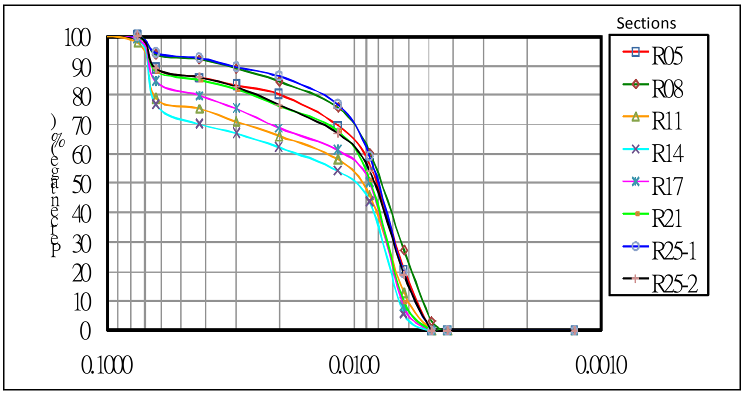

Figure 3 Sediment size distributions (No. is from dam to upstream)

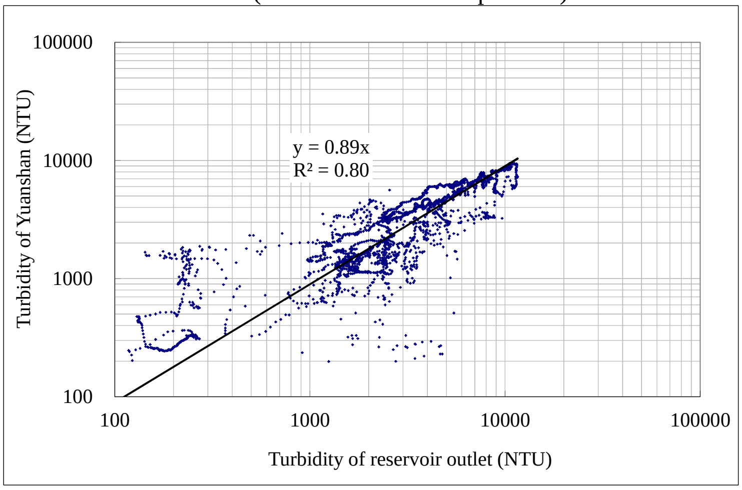

Figure 4. Sediment concentration relationship between reservoir and Yuanshan weir

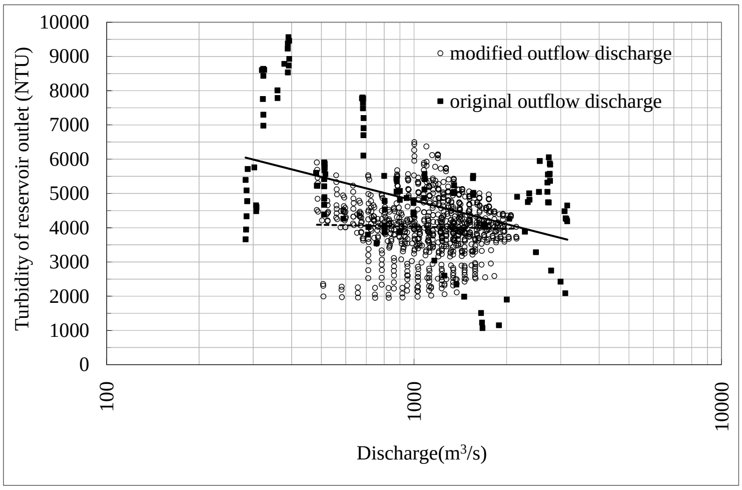

Figure 5. Effect of sediment concentration due to various outflow discharges of tunnel spillway

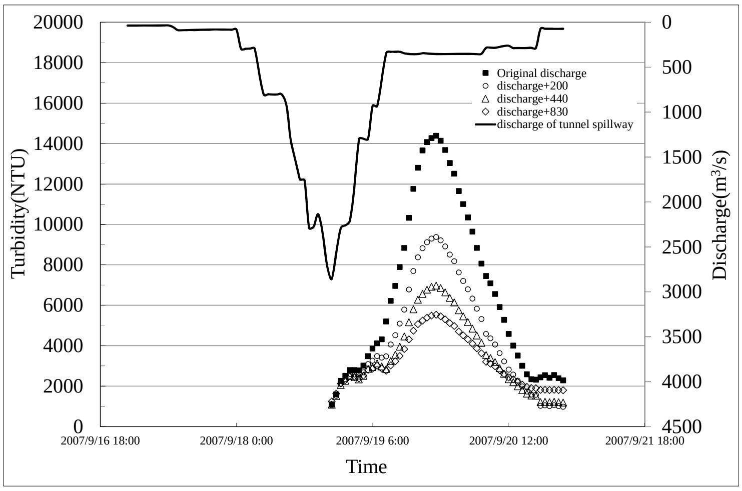

Figure 6. Sediment concentration decrease using clear water during Typhoon Wipha

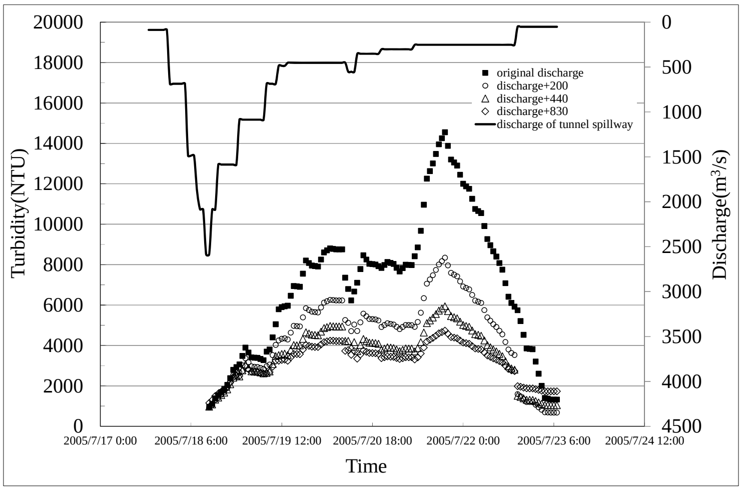

Figure 7. Sediment concentration decrease using clear water during Typhoon Haitang